with a 12.7 mm (½ in) CFRP bar, the effect of bar diameter on transfer length has already been examined by Mahmoud et al. (1999), and the authors expect that bar diameter will have an effect similar to the one established in that previous study.

Flexural test results

Modes of failure —two modes of failure were recorded: bond pullout failure and bar rupture failure. The bar rupture failure mode is easily defined and is distinguishable from other types of failure: the prestressed bar suddenly ruptures, and the applied load drops instantly to zero. This type of failure was also associated with a loud "ping" cracking sound. Bond pullout failure is defined when a slippage of 0.25 mm (0.01 in) is recorded at the unloaded end of the prestressed bar. This limit has been set by ASTM A882/A882M (1992) and has been used by other researchers (Zaki et al. 1996). When the bar pullout was initiated, a loud noise could be heard, and the applied load dropped to a lower value (residual strength). The noise continued as long as the beam was able to resist loading at the reduced stiffness. After flexural tests, selected beam specimens were cut transversely and longitudinal at selected locations and inspected visually, Figure 10 and 11. This autopsy revealed two main findings. First, bond failure occurred between the sand coating layer and the fibre interface of the CFRP bar. Second, the slippage was initiated within the transmission zone when the bond stress waves resulting from the loading approached the CFRP bar in the transmission zone. Failure due to bar rupture typically occurred within the constant moment region or, less commonly, under one of the applied load points. In the case of bond failure, the flexural crack closest to the end of the transfer zone continued to widen significantly during the slippage of the CFRP bar from the concrete. It was later determined that this crack forms a boundary line of the failed bond region.

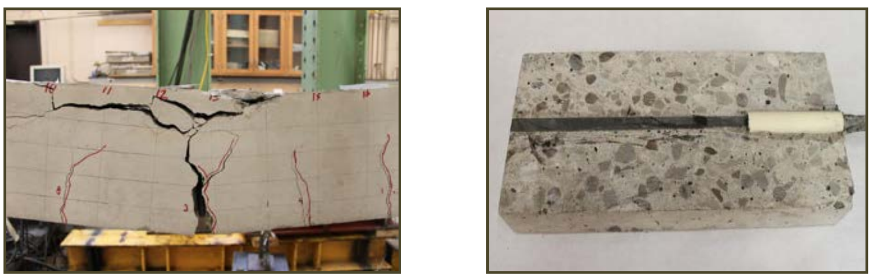

(a) Midspan bar rupture failure

(b) Concrete slice showing the CFRP bar still in complete contact with the concrete

Figure 10— Bar rupture mode of failure for beam S45-4

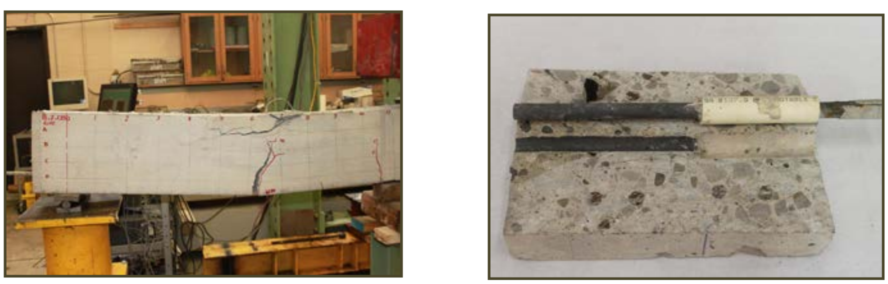

(a) Pullout bond failure at the end of the transmission zone

(b) Cut-off slices showing the bond failure

Figure 11— Pull out bond failure for beam S60-2

Moment-deflection responses— Table 3 provides a summary of the flexural test results. It should be noted that the deflection values exclude camber values and that the moment does not include moment due to the beam's own weight. Two beams exhibited combined modes of failure: S30-2 and S60-4. In these beams, the failure began as pullout; however, during slippage, the beam was able to withstand an additional load, resulting in bar rupture. Beam S30-4 exhibited a premature bar rupture mode of failure: the CFRP bar ruptured at low tensile stresses. This beam is one of the two beams that produced bar-cracking noises during the prestressing operation. The results for this beam are not discussed further and are excluded from the bond stress analysis.

Table 3— Flexural test results

Group/ Beam label		Shear span, mm	Failure		Type of failure
			Moment, kN.m	Deflection, mm	
I	S30-1	1100	16.7	11.9	Pullout
	S30-2	1250	42.4	69.2	Rupture
	S30-3	1350	33.9	52.5	Pullout/Rupture
	S30-4	1500	17.8	25.4	Rupture*
II	S45-1	1100	34.0	35.9	Pullout
	S45-2	1250	36.8	35.7	Pullout
	S45-3	1350	36.9	31.5	Pullout
	S45-4	1500	43.5	40.6	Rupture
III	S60-1	1100	26.3	12.9	Pullout
	S60-2	1350	31.4	19.2	Pullout
	S60-3	1500	26.7	21.2	Pullout
	S60-4	1700	33.2	22.3	Pullout/Rupture
IV	N30-1	1350	42.3	68.8	Rupture
	N60-2	1250	29.4	12.5	Pullout
	N60-3	1350	44.6	48.5	Rupture
	N60-4	1500	43.7	49.4	Rupture

* This beam failed by premature bar rupture failure.
1.0 kN.m = 740 lb.ft, 1 mm = 0.0393 in

In general, the moment-deflection response of all beams was bilinear behavior with a smooth transition between the two segments. Figures 12 to 15 show the flexural test results. The initial linear part of the curve was characterized by a steep slope, which corresponds to the uncracked stiffness. As expected, the average cracking moment increased as the prestressing level increased. As the loading increased, the flexural cracks propagated upward slowly due to the prestressing effect.

Figure 12 shows the test results for Group I. Beam S30-1, with a shear span of 1100 mm, was subject to bond failure at an applied moment of 16.7 kN.m (12.4 kips.ft). When the shear span was increased to 1250 mm (49 in), beam S30-2 failed due to bar rupture at an applied moment of 33.9 kN.m (25.1 kips.ft). This moment represented less than the predicted section capacity, yet the bar ruptured at a tensile stress less than the guaranteed tensile strength. When the shear span was increased to 1350 mm (53 in), the beam was able to hold up to the level of section capacity; however, the bar slipped at a tensile stress very close to the guaranteed tensile strength. The test results for Group I suggest that the development length should be between 1350 mm (53 in) and 1500 mm (59 in).

The Group II results followed the expected trend: the moment capacity increased as the shear span was increased, Figure 13. The first three beams, S45-1, S45-2, and S45-3, failed due to bond pullout, and the moment increased from 34.0 kN.m (25.0 kips.ft) to 39.0 kN.m 28.8 (kips.ft)when the shear span was expanded from 1100 mm (43.3 in) to 1350 mm (53.0 in). Beam S45-4, with a shear span of 1500 mm (59 in), failed by bar rupture at an applied moment of 43.5 kN.m (32.1 kips.ft). The test results for Group II suggest that the development length should be very close to 1500 mm (59 in).

In Group III (Figure 14), beams S60-1, S60-2, and S60-3 failed due to pullout bond failure while beam S60-4 exhibited combined bond/flexure failure.. This beam also displayed noticeable loss of stiffness when the moment exceeded 38 kN.m(28.1 kips.ft). No end slip was recorded at this moment. A possible explanation for this response is the occurrence of local slippage within the transmission zone. The test results suggest that the development length for CFRP bar at 60% prestress level above 1700 mm (67 in).

Group IV beams has one beam (N30-1) prestressed to 30 % and the other three prestressed to 60 %. Figure 15 shows the flexure test results of this group. Beam N30-1 failed due to bar rupture at an applied moment of 43.6 kN.m (32.2 kips.ft). With a shear span of 1250 mm (49.0 in), beam N60-2 exhibited bond pullout failure at an applied moment of

29.4 kN.m (21.7 kips.ft). Beam N60-4 failed by bar rupture at an applied moment of 44.6 kN.m (32.7 kips.ft). No improvement in failure moment was recorded when the shear span was increased to 1500 mm (59 in).

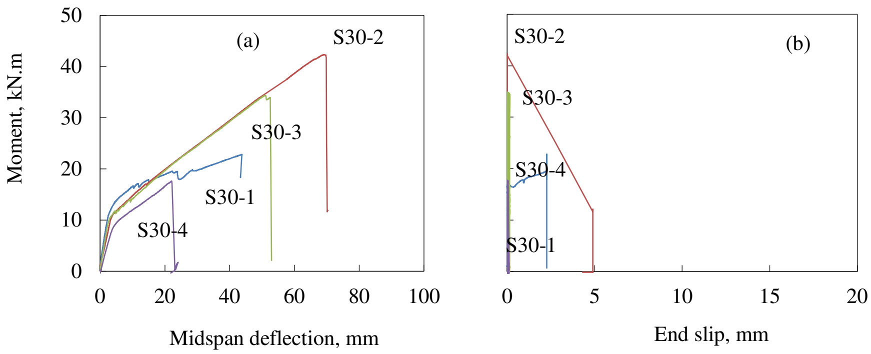

Figure 12— Flexural test results for Group I: (a) Moment-deflection; (b) Moment-end slip

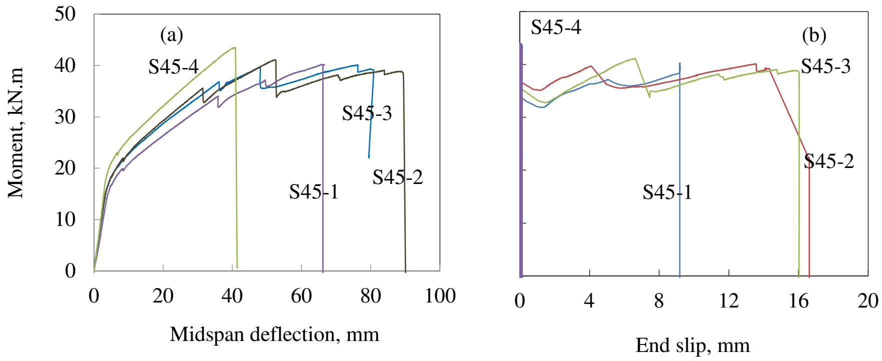

Figure 13— Flexural test results for Group II: (a) Moment-deflection; (b) Moment-end slip

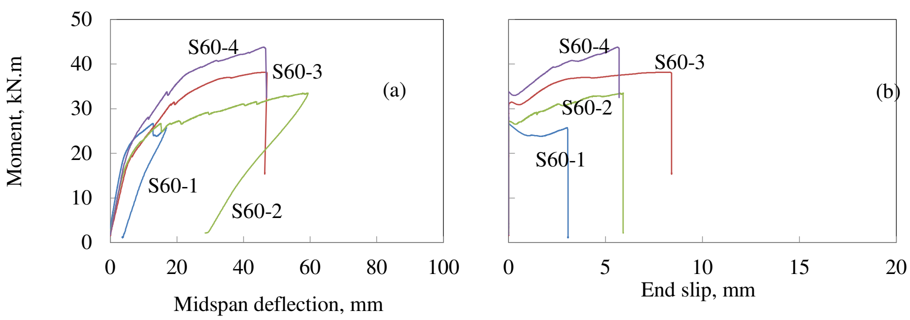

Figure 14— Flexural test results for Group III: (a) Moment-deflection; (b) Moment-end slip

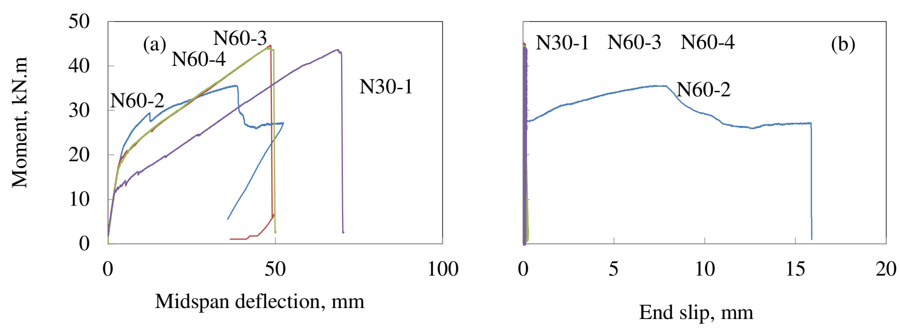

Figure 15— Flexural test results for Group IV; (a) Moment-deflection; (b) Moment-end slip

1.0 kN.m = 740 lb.ft, 1 mm = 0.0393 in

<u>Longitudinal tensile stress development and bond stress profile</u>

During the flexural test, tensile stress development in the CFRP bars was monitored by means of strain gauges, which were distributed along the transfer length and the flexural bond length. The tensile stress and bond stress development within the shear span were calculated based on the strain measurements. Figure 16 shows the tensile and bond stress profiles of a typical beam that failed by bond pullout, beam S45-3. For this particular beam, when slip began at an applied moment of 32.8 kN.m (24.2 kips.ft), the tensile stress dropped to nil at the first strain gauge location (150 mm, 6 in, from the support), indicating that the bar was debonded at that location. As the load increased, the reduction in the tensile stress in the bar progressed toward the midspan of the beam, indicating further debonding. The bond stress followed a similar pattern, with no increase in bond stresses within the transfer zone due to flexural loading. When the load reached the peak (35.5 kN.m, 26.2 kips.ft), the CFRP bar was unable to withstand any bond stresses within the transfer zone in order to resist the applied moment, and the beam displayed bond pullout failure. Initially, the bond stress peaked close to the free end of the beam and then dropped linearly toward the midspan. As the load was increased and slip was initiated, the peak bond stress moved inward, with further debonding of the CFRP bar within the transfer zone at the onset of failure. This finding explains the observable failure cracks. All of the beams exhibited bond pullout failure, with the failure cracks being located very close to the end of the transfer zone.

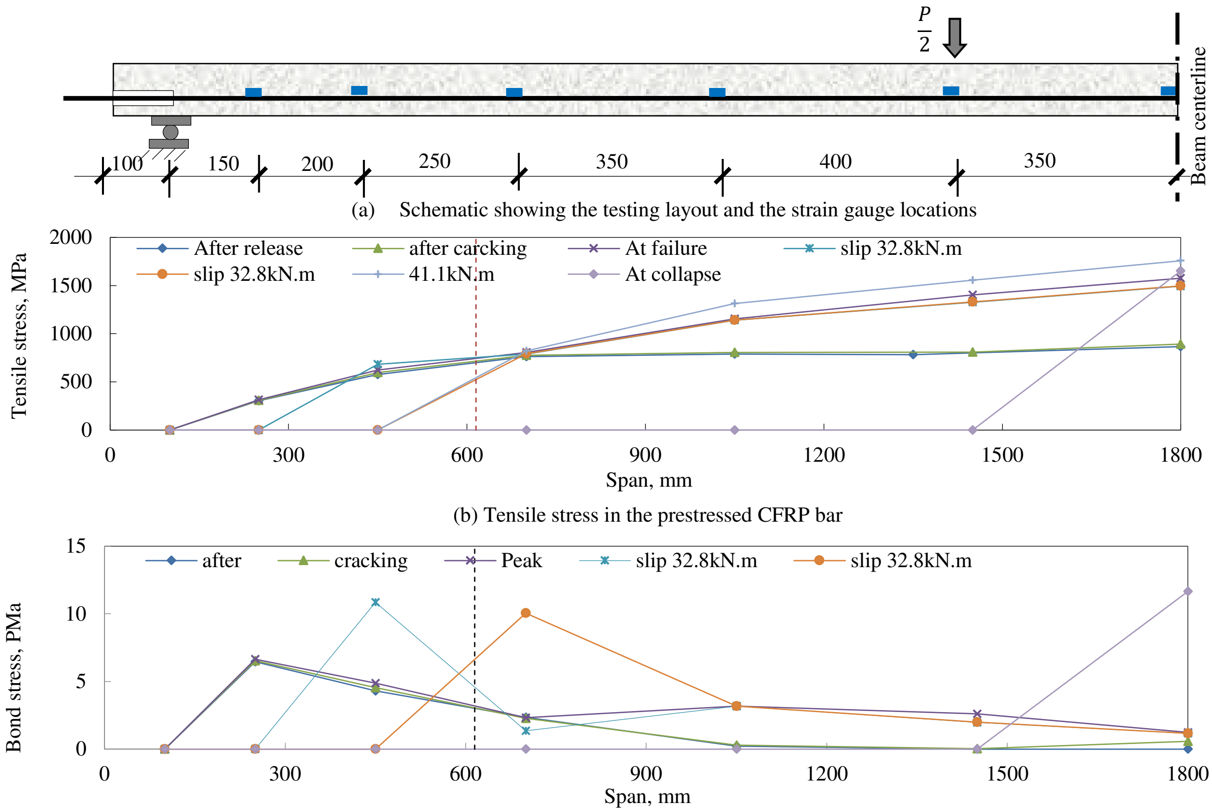

(a) Schematic showing the testing layout and the strain gauge locations

(b) Tensile stress in the prestressed CFRP bar

(c) Bond stress development due to prestress release and flexural testing

Figure 16— Tensile and bond stress development in the prestressed CFRP bars during the flexural test of beam S45-3: shear span is 1350 mm (bond pullout mode of failure)

1.0 kN.m = 740 lb.ft, 1 MPa = 145 psi, 1 mm = 0.0393 in

Figure 17 shows the tensile stress and bond stress profiles for beam S45-4, which failed by bar rupture. No increase in tensile or bond stress in the CFRP bar occurred within the transfer zone due to flexural loading; however, the tensile stresses in the CFRP bar continued to increase within the flexural bond length. The flexural length available in this beam was sufficient to enable the bond stresses to provide the required anchorage for the additional tensile stress development, and the prestressed CFRP bar survived to the point of rupture. The beams made with NVC followed a similar pattern; however, the bond stress values were slightly higher, and the rupture of the CFRP bars occurred at a shorter embedment length.

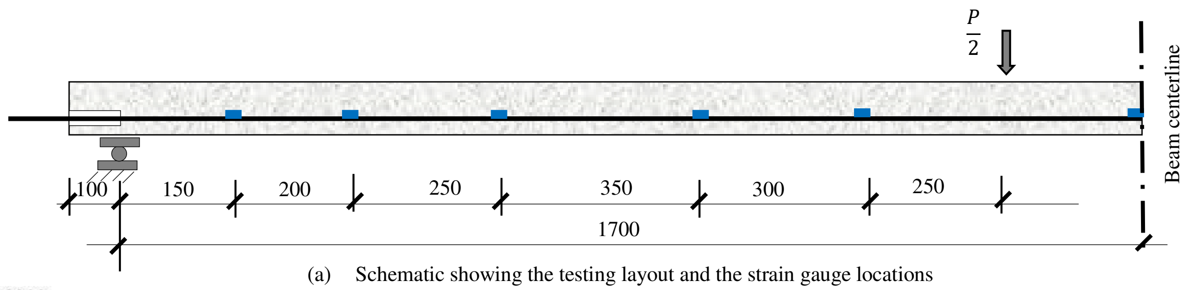

(a) Schematic showing the testing layout and the strain gauge locations

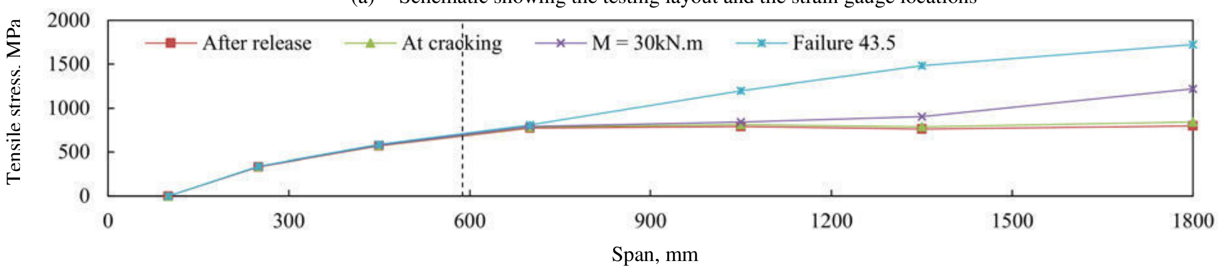

(b) Tensile stress in the prestressed CFRP bars

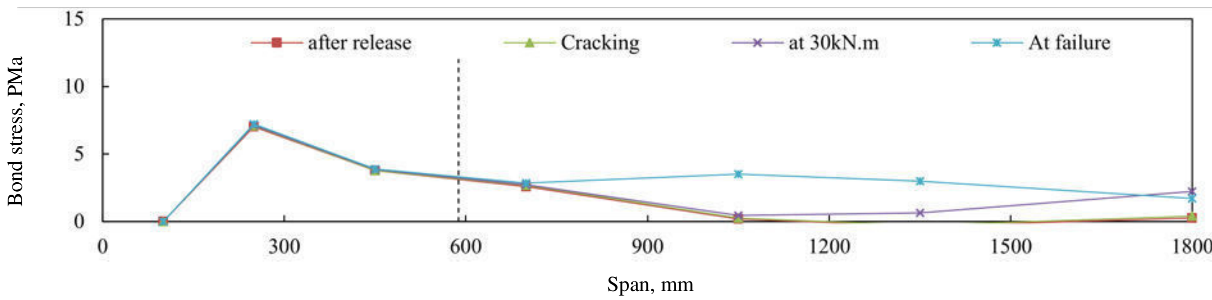

(c) Bond stress development due to prestress release and flexural testing

Figure 17— Tensile and bond stress development in the prestressed CFRP bars during the flexural test of beam S45-4: shear span is 1500mm, and the beam exhibited bar rupture failure

1.0 kN.m = 740 lb.ft, 1 MPa = 145 psi, 1 mm = 0.0393 in

Average bond stress within the flexural bond length

The increase in tensile stress in the prestressing CFRP bars due to load is defined as the flexural tensile stress. The average bond stresses in the flexural bond region were calculated based on the flexural tensile stress and the available flexural bond length. Table 4 lists the available flexural bond length, the increase in tensile stresses due to flexural load, and the calculated average bond stresses. The results indicate that the flexural bond stresses were significantly less than the average bond stress that developed within the transfer zone. The table also provides the average flexural bond stress normalized to the concrete compressive strength raised to the power of 0.67.

The normalized bond stress values were plotted against the flexural tensile stress values for the prestressed CFRP bars, Figure 18. Only beams that failed by bond pullout were included in this plot. The relationship indicates that the normalized bond stress increased as the flexural tensile stress rose. It is important to note here that higher tensile flexural stresses are associated with longer flexural bond length: beams with a longer flexural bond length have a greater margin for developing flexural tensile stress before the bond stress waves reach the transmission zone. The SCC specimens showed normalized average bond stresses similar to those of the NVC beams. A linear relationship between the normalized flexural bond stress and the flexural tensile stresses in a prestressed CFRP bar in SCC can be formulated as shown in Eqn. (8). This relationship represents the best fit of the data, with an R^2 of 0.79. The equation is bounded by bond pullout failure because the available concrete cover was sufficient to prevent splitting bond failure.

$$\frac{u_f}{f_{ci}^{0.67}} = 1.0 \times 10^{-4} f_f + 0.0934 \qquad (8)$$

where f_f is the flexural bond stress, MPa; u_f is the flexural average bond stress, MPa; and f'_c is the compressive strength of the concrete, MPa.

Table 4— Flexural bond stress of CFRP prestressed beams

Beam	f_e, MPa	l_{tr}, mm	Shear span, mm	Available l_f, mm	Increase in tensile stress, MPa	Average u_f, MPa	$\frac{u_f}{f_c'^{0.67}}$
S30-1	550	306.0	1100	794.0	810	3.2	0.19
S30-2	535	301.8	1250	943.0	1166	3.9	0.24
S30-3	626	337.0	1350	1013.0	1216	3.8	0.28
S30-4	605	320.0	1500	1180	583	*	*
S45-1	750	533.5	1100	566.5	582	3.4	0.19
S45-2	794	515.8	1250	751.8	715	2.9	0.17
S45-3	777	514.5	1350	835.5	636	2.7	0.16
S45-4	742	487.0	1500	1013.0	927	2.9	0.17
S60-1	933	668.5	1100	434.0	370	2.7	0.16
S60-2	995	732.5	1350	617.5	479	2.5	0.15
S60-3	920	661.8	1500	838.2	611	2.3	0.17
S60-4	974	671.8	1700	1028.2	814	2.5	0.18
N30-1	540	274.8	1350	1075.2	1291	3.8	0.23
N60-2	890	526.5	1250	723.5	540	2.4	0.15
N60-3	833	545.4	1350	804.6	791	3.1	0.19
N60-4	1076	534.1	1500	965.9	806	2.6	0.16

* This beam failed by premature bar rupture, and its test results were excluded from the average bond stress analysis.
1 MPa = 145 psi, 1 mm = 0.0393 in

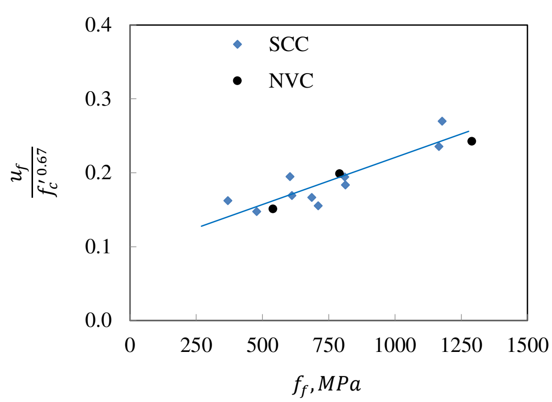

Figure 18— Normalized bond stress versus flexural tensile stress for a CFRP bar
1 MPa = 145 psi

Flexural bond length equation

The flexural bond equation can be formulated based on the basic principle of the equilibrium condition of tensile stresses in the reinforced prestressed bars and the surrounding bond stresses. The equilibrium of the forces between two sections of a beam under flexural loading can be written as follows:

$$\Delta T = \mu_f \; \pi \; d_b \; \Delta l \tag{9}$$

where ΔT is the change in the tensile force in the CFRP bar over the length of Δl *(mm)*, N; u_f is the average bond stress between these two sections, MPa; and d_b is the diameter of the CFRP bar, mm.

Replacing distance Δl by the available flexural bond length (l_f) of a beam enables Eqn. (9) to be rewritten as

$$T_f = \mu_f \ \pi \ d_b \ l_f \tag{10}$$

where T_f is the flexural tensile force in the prestressed CFRP bar at the end of the flexural bond length, N; u_f is the average flexural bond stress; and l_f is the available flexural bond length. Eqn. (10) assumes that the full flexural tensile stress in the prestressing bars will be anchored within the flexural bond length. No bond stresses beyond the flexural bond length are accounted for.

Solving Eqn. (8) and Eqn. (10) for l_f gives a relationship between the flexural tensile stress and the flexural bond length required to accommodate the flexural stress without bond pullout failure:

$$l_f = \frac{(f_{frpu} - f_{pi}) \, d_b}{\alpha_f \ f_c^{i \ 0.67}} \tag{11}$$

and

$\alpha_f = 0.37 + \frac{(f_{frpu} - f_{pi})}{2500}$ in N-mm units and equal to $0.20 + \frac{(f_{frpu} - f_{pi})}{690}$ in inch-pound units.

where f_{frpu} is the tensile rupture stress of the CFRP bar, MPa; f_{pi} is the initial prestress, MPa; and α_f is the coefficient of flexural bond length.

The equation determines the minimum flexural bond length required in order for the prestressed CFRP bar to withstand the tensile stresses to the point of rupture. The equation can also be used to determine the maximum permissible tensile stress of a prestressed CFRP bar for a given flexural bond length. Table 5 enables a comparison of the experimental flexural bond lengths: those predicted according to the ACI440.4R-04 equation and those produced by the proposed model, as expressed in Eqn. (11).

Table 5— Comparison of the experimental data, ACI predictions, and the proposed model predictions for flexural bond length of the CFRP bars in the SCC specimens

Group/ Beam labels		Experimental		ACI 440.4 prediction		Proposed model	
		f_f, MPa	l_f, mm	l_f, mm	Prediction/ Exp	l_f, mm	Proposed / Exp
I	S30-1	811	794.0	617.4	0.78	884.5	1.11
	S30-2	1166	943.3-	889.0	0.94	1057.6	1.12
	S30-3	1216	1013.0	1128.7	1.11	1294.2	1.28
	S30-4	-	-	-	-	-	-
II	S45-1	604	566.5	441.3	0.78	716.9	1.27
	S45-2	687	751.8	501.6	0.67	773.4	1.03
	S45-3	710	835.5	518.8	0.62	788.6	0.94
	S45-4	-	-	-	-	-	-
III	S60-1	370	434.0	281.6	0.65	539.7	1.24
	S60-2	479	617.5	364.8	0.59	645.1	1.04
	S60-3	611	838.2	567.6	0.68	917.7	1.09
	S60-4	814	1028.2	755.4	0.73	1008.1	1.05

1 MPa = 145 psi, 1 mm = 0.0393 in

The ACI prediction values were unconservative by a range of 20 % to 40 %, possibly because the ACI equation is based on the assumption of a constant bond stress within the flexural bond length irrespective of the flexural tensile stress in the prestressed bar. The experimental results for this study demonstrated that the average flexural bond stress is a function of the flexural tensile stresses. High values of flexural tensile stress would be expected when longer flexural bond lengths are available because a longer flexural bond length is associated with a more extensive uncracked portion of the beam and is not subject to transfer bond stresses. The ability of the proposed model to vary the coefficient (α_f) enabled the change in flexural bond stress to be addressed. The predicted results calculated by the proposed model correlate well with the experimental findings: the ratio of the proposed to the predicted results ranged from 0.94 to 1.28, with a mean value of 1.12.

Development length of prestressed CFRP bars in SCC beams

The development length can be calculated by adding the transfer length (Eqn. 7) and the flexural bond lengths (Eqn. 11). The total development length of a prestressed CFRP bar in SCC is given by the following:

$$l_d = \frac{f_{pi}\, d_b}{\alpha_t\, f_{ci}^{0.67}} + \frac{(f_{frpu} - f_{pi})\, d_b}{\alpha_f\ \ f_c^{i\ 0.67}} \qquad (12)$$

where $\alpha_t = 2.84 - \frac{f_{pi}}{912}$ and $\alpha_f = 0.37 + \frac{(f_{frpu} - f_{pi})}{2500}$ in N-mm units, and

$\alpha_t = 1.45 + \frac{f_{pi}}{250}$ and $\alpha_f = 0.20 + \frac{(f_{frpu} - f_{pi})}{690}$ in inch-pound units

Table 6 provides a comparison of the development length results with the predictions based on the ACI 440.4R-04 equation and those produced by the proposed model. The ACI prediction of the development length is clearly in good agreement with the results for the specimens in which the CFRP bar was prestressed to 30 %; however, when the prestressing was increased above 45 %, the ACI prediction was unconservative by up to 25 % on average. The predictions of the development length provided by the proposed model were in good agreement with the experimental values. The ratio of the predicted to the experimental development lengths ranged from 0.95 to 1.21. The average predicted-to-experimental ratio was 1.08, with a standard deviation of 0.078.

The predicted results based on the proposed model correlate well with the experimental results obtained. However, the proposed equation might need further verification when additional data become available. Although this equation is based on the experimental results obtained with a 12.7 mm CFRP bar only, the effect of bar diameter on transfer length has already been examined by Mahmoud et al. (1999), and the authors expect that bar diameter will have an effect similar to the one established in that previous study.

Table 6— Comparison of the experimental, ACI prediction and the proposed model of the development length.

Group/ Beam labels		Experimental		ACI 440.4 prediction		Proposed model	
		l_e, mm	Total stress, MPa	l_d, mm	ACI/Exp	l_d, mm	Proposed / Exp
I	S30-1	1100.0	1359.9	1003.0	0.91	1230.6	1.12
	S30-2	1250.0	1701.1	1263.8	1.01	1391.4	1.11
	S30-3	1350.0	1841.9	1488.1	1.10	1630.5	1.21
	S30-4*	1500.0	-	-	-	-	-
II	S45-1	1100.0	1354.0	913.0	0.83	1188.1	1.08
	S45-2	1250.0	1480.5	1004.4	0.80	1290.7	1.03
	S45-3	1350.0	1486.4	1010.5	0.75	1289.0	0.95
	S45-4*	1500.0	-	-	-	-	-
III	S60-1	1100.0	1302.2	933.3	0.85	1273.8	1.16
	S60-2	1350.0	1473.9	1060.9	0.79	1464.1	1.08
	S60-3	1500.0	1531.5	1097.7	0.73	1512.5	1.01
	S60-4	1700.0	1787.6	1312.4	0.77	1725.4	1.01

1 MPa = 145 psi, 1 mm = 0.0393 in

CONCLUSIONS

Sixteen prestressed beams with CFRP bars were fabricated and tested with respect to transfer length and flexural bond length. Twelve beams were made from SCC and four from NVC. The prestressing level was varied from 30% to 60% of the guaranteed rupture tensile stress of CFRP bars. All beams were tested for transfer length of the CFRP bars immediately after prestressing load release. Four-point flexural test were carried on all beams at 28 days or thereafter to evaluate for flexure bond length and development length. Based on the test results, the following conclusions can be drawn:

1) The bond stresses between SCC and prestressed CFRP bars at transfer were less those of NVC at a similar age. However, the bond stresses for both types of concrete were similar at later ages.
2) The ACI 440.4R-04 equation for the transfer length of CFRP bars provides a close correlation with the measured transfer length of 12.7 mm (½ in) CFRP bars in SCC at a 30 % prestress level, but when the initial prestressing exceeded 750 MPa(110 ksi), the ACI440.4R-04 underestimated the transfer length.
3) The beams with a shear span less than their development length that were tested for flexural bond length exhibited slippage of the prestressed CFRP bar within the transfer zone. The slip was recorded at the unloaded end, but the beams were able to sustain a portion of the load during the slippage. The slippage began when the action of the flexural bond stress reached the transmission zone. The failure mechanism was bond demand exceeding bond strength at the transmission zone and a shift in the transmission zone toward the midspan of the beam. Beams collapsed when the residual bond stress was no longer sufficient to accommodate the tensile stress in the prestressed bars. The interface between the sand coating and the fiber was proven to be the critical bond interaction in this type of CFRP bar.
4) The ACI440.4R-04 guideline provided relatively accurate predictions of the development length of the 12.7 mm CFRP bars prestressed to 30 % but underestimated the development length by about 25 % and 40 % with respect to prestressing levels of 45 % and 60 %, respectively. On the other hand, ACI440.4R-04 provided good correlation at all prestress levels for beams made from NVC.
5) A new modification was proposed to the constant coefficients (α_t and α_f) in the existing ACI440.4R-04 equations to account for SCC. The results correlate well with the measured experimental data. The ratio of the average value calculated by this modification to the measured development length is 1.08, with a standard deviation of 0.078. However, calibration of the proposed change vis-à-vis independent work would prove beneficial in order to refine its applicability for a wider variety of CFRP bars.

ACKNOWLEDGEMENTS

The first author gratefully acknowledges the University of Tripoli in Libya for providing a scholarship. The financial support provided by NSERC is also acknowledged. The support of the technical staff at the University of Waterloo is greatly appreciated.

REFERENCES

ACI Committee 237 (2007), “Self-Consolidating Concrete,” *ACI 237R-07,* American Concrete Institute, Farmington Hills, MI, USA.

ACI Committee 440 (2004), “Pre-stressing Concrete Structures with FRP Tendons,” ACI 440.4R-04, American Concrete Institute, Farmington Hills, MI.

Burgueno, R., and Haq, M. (2007), “Effect of SCC Mixture Proportioning on Transfer and Development Length of Prestressing Strand,” American Concrete Institute, SP- 247-9, 105-116.

Domenico, N., Mahmoud, Z., and Rizkalla, S. (1998), “Bond Properties of Carbon Fiber Composite Prestressing Strands,” ACI Str. J., 95(3), 281-290.

Girgis, A., and Tuan, C., (2005). “Bond Strength and Transfer Length of Pretensioned Bridge Girders Cast with Self-Consolidating Concrete.” PCI Journal 50(6), 72-87.

ISIS Canada (2008). “Prestressing Concrete Structures with Fiber Reinforced Polymers.” Design Manual No. 5, Winnipeg, Manitoba, Canada.

Janney, J. (1954). “Nature of Bond in Pretensioned Concrete.” ACI Journal, 25(9), 717-736.

Khayat, K., and Mitchell, D., (2009). “Self-Consolidating Concrete for Precast, Prestressed Concrete Bridge Elements.” NCHRP report 628, Transportation Research Board, Washington, D.C. USA.

Krem, Slamah, (2013) “Bond and flexural behaviour of self-consolidating concrete beams reinforced and prestressed with FRP bars”, *Doctoral dissertation, University of Waterloo*

Logan, D., (1997), "Acceptance Criteria for Bond Quality of Strand for Pretensioned Prestressed Concrete Applications," PCI J., 42(2), 52-90.

Mahmoud, Z., Rizkalla, S., and Zaghloul, E., (1999), "Transfer and Development Lengths of Carbon Fiber Reinforced Polymers Prestressing Reinforcement," ACI Str. J., 96(4), 594- 602.

Marti-Vargas, J., Arbelaez, C., Serna-Ros, P., and Castro-Bugallo, C. (2007). "Reliability of Transfer Length Estimation from Strand End Slip." ACI Structural Journal, 104(4), 487-494.

Naito, C., Parent, G. and Brunn, G. (2006). "Performance of Bulb-Tee Girders Made with Self-Consolidating Concrete." PCI Journal, 51(6), 72-85.

Pozolo, A. M., and Andrawes, B. (2011). "Transfer length in Prestressed Self-Consolidating Concrete Box and I-Girders." ACI Structural Journal, 108(3), 341-349.

Russell, B., and Burns, N. (1996). "Measured Transfer Length of 0.5 and 0.6 in Strands in Pretensioned Concrete." PCI Journal, 41(5), 44-65.

Schindler, A. et al., (2007), "Properties of Self-Consolidating Concrete for Prestressed members," ACI Mat. J., 104(1), 53-61.

Soudki, K. (2010). "Tensile Capacity of CFRP V-Rod Bars." Technical Report, University of Waterloo, Waterloo, Ontario, (May 3rd 2010).

Taerwe, L., and Pallemans, I. (1995). "Force Transfer of AFRP Bars in Concrete Prisms." *Proc., .2nd Int. Symp.on Non-metallic (FRP) Reinforcement for Concrete Structures,* RILEM, Ghent, Belgium, 54-163.

Vilanova, A., Fernández-Gómez, J., and Landsberger G., (2012), "Mechanical Properties of Self-Consolidating Concrete Using Conventional Concrete Models," ACT Str. J., 109(6) 587-596.

Zou, P. (2003). "Long-Term Properties and Transfer Length of Fiber-Reinforced Polymers." Journal of Composites for Construction, 7(1), 10-19.

NOTATIONS

l_t is the transfer length
f_{pi} is the initial prestressing stress in prestressing bar
d_b is the prestressing bar diameter
α_t is a coefficient that accounts for the type of bar material
f_{pu} is the ultimate rupture strength of the prestressing bar
f_{pe} is the effective prestress in the prestressing bar
α_f is a coefficient that is dependent on the surface condition
ε is the strain measured in the concrete beam at the level of the prestressed bar, and the symbol (i-1, i, i+1) represents the Demec points along the beam.
Δ is the measured end slip of the prestressing bar due to prestress force release
E is the modulus of elasticity of the prestressing bar
u is the average bond stress
f_{ci} is the concrete compressive strength at prestress stress release.
T_{pi} is the prestressing force
f_f is the tensile stress in prestressing bar due flexural load
u_f is the flexural average bond stress
f'_c is the compressive strength of the concrete
ΔT is the change in the tensile force in the prestressing bar over a length of Δl
T_f is the flexural tensile force in the prestressing bar at the end of the flexural bond length
l_f is the available flexural bond length
f_{frpu} is the tensile rupture stress of the CFRP bar